 ©2011 Kvantovaya Elektronika and Turpion Ltd

PACS numbers: 61.80.Ba; 42.62.–b; 42.79.Dj
DOI: 10.1070/QE2011v041n07ABEH014528

Study of the spatial resolution of laser thermochemical technology for recording diffraction microstructures

V.P. Veiko, V.I. Korol'kov, A.G. Poleshchuk, A.R. Sametov, E.A. Shakhno, M.V. Yarchuk

Abstract**. The thermochemical method for recording data, which is based on local laser oxidation of a thin metal film with subsequent etching of the unirradiated region, is an alternative to laser photolithography and direct laser removal of the film material. This recording technology is characterised by the absence of thermal and hydrodynamic image distortions, as in the case of laser ablation, and the number of necessary technological operations is much smaller as compared with the photomask preparation in classical photolithography. The main field of application of the thermochemical technology is the fabrication of diffraction optical elements (DOEs), which are widely used in printers, bar-code readers, CD and DVD laser players, etc. The purpose of this study is to increase the resolution of thermochemical data recording on thin chromium films.**

Keywords*: laser thermochemical technology, data recording, thin films, diffraction optical elements.*

1. Introduction

A number of methods for fabricating microstructures on thin films are based on the thermal effect of laser radiation. A specific feature of the laser thermochemical technology (LTT) is that the laser-induced heating of a thin metal (in particular, chromium) film gives rise to chemical and physical processes, which are localised within the heated region of the film; i.e., a hidden thermochemical image is formed [1]. The physical and chemical compositions in the hidden-image region differ from those of the initial film; hence, the image structure can be revealed using wet chemical etching (development) [1, 2].

Application of LTT is most appropriate for the fabrication of diffraction optical elements (DOEs) [3] of amplitude type, which generally consist of opaque bands (diffraction zones) of variable width and period. The reason is that in some cases a diffraction structure must be formed on convex or concave optical surfaces or substrates of large thickness and area [4]. These specific features limit the application of the standard photolithography [5] (which is based on photoresists) to fabricate precise and large DOEs. The point is that the only way to obtain a thin uniform photoresist film is centrifugation, which can hardly be applied to heavy substrates. Obviously, the thermochemical formation of DOE structure in thin chromium films allows one to simplify significantly the DOE fabrication and increase its accuracy [6].

According to the classical model [1], the laser-induced heating of thin chromium films leads to the formation of a thin oxide layer in them, which changes the physical and chemical properties of the irradiated surface. It was also found [1, 2, 7] that the formation of a chromium oxide film on the surface is accompanied by some other processes, in particular, annealing, recrystallisation, and partial oxidation of the film throughout its thickness. Thus, laser irradiation of a chromium film both initiates the processes of surface oxidation and changes the bulk film properties. However, laser-initiated surface oxidation appears to play the dominant role in the formation of microstructures in chromium films in the irradiation regimes studied. The LTT based on the irradiation of a substrate coated by a thin chromium film and rotating at a constant speed and its subsequent chemical treatment in a selective etchant became most widespread. The exposure is performed by focused radiation of a high-power cw laser at a circular (or helical) motion of the substrate using a laser recording system [8]. This method was used to fabricate unique DOEs, intended, in particular, for monitoring the shape of aspherical mirrors of the telescopes largest in the world [4] with minimum sizes of chromium structure of about 500 nm and a total size of the elements as large as 230 mm.

In the recent years, the interest in the diffraction elements operating in the UV and VUV ranges, as well as the need for subwave DOEs, has sharply increased [9, 10]. In this context, a problem of increasing the spatial resolution of laser recording on chromium films has arisen [11]. In this paper, we report the results of the theoretical and experimental study of the possibilities (and limitations) for increasing the LTT resolution.

2. Statement of the problem

Let us consider the oxidation of a thin metal film heated by laser radiation. Upon heating, a number of physicochemical processes are activated in the film, in particular, oxygen

V.P. Veiko, E.A. Shakhno, M.V. Yarchuk St. Petersburg State University of Information Technologies, Mechanics, and Optics, Kronverkskii prosp. 49, 197101 St. Petersburg, Russia; e-mail: veiko@lastech.info.ru;
V.I. Korol'kov, A.G. Poleshchuk, A.R. Sametov Institute of Automation and Electrometry, Siberian Branch, Russian Academy of Sciences, prosp. Akad. Koptyuga 1, 630090 Novosibirsk, Russia

Received 30 December 2010; revision received 29 March 2011
Kvantovaya Elektronika **41** (7) 631 – 636 (2011)
Translated by Yu.P. Sin'kov

adsorption on the surface, diffusion of metal and oxygen ions, metal oxidation with the formation of an oxide layer, etc.) [12]. The rate of the increase in the oxide layer thickness H as a function of temperature T is determined by the ratio of the rates of the aforementioned processes. Under isothermal heating the oxidation kinetics is limited by the slowest stage: diffusion. In this case, it is described by the Wagner equation

$$\frac{\mathrm{d}H}{\mathrm{d}t} = \frac{B}{H}\exp\left(-\frac{T_\mathrm{a}}{T}\right), \quad (1)$$

where B is the constant of the parabolic oxidation law, T_a is the activation energy of the diffusion processes (in kelvins), and t is time.

To calculate the oxide layer thickness under nonisothermal laser oxidation, we will use the approach developed by M.N. Libenson. According to this approach, if the film temperature is much lower than T_a, the activation exponential sharply increases with an increase in temperature, and the main contribution to the increase in the oxide film thickness occurs at the instants when the temperature T is close to the maximum value T_max. Hence, one can determine the oxide layer thickness under laser heating as the oxide layer thickness under isothermal heating for some equivalent time (shorter than the irradiation time) t_eq [13]:

$$H = \sqrt{2B\exp\left(-\frac{T_\mathrm{a}}{T_\mathrm{max}}\right)t_\mathrm{eq}}. \quad (2)$$

The t_eq value is determined by the character of the change in temperature with time during laser irradiation. In particular, if the maximum temperature is reached at an instant t_0 before the end of this process, t_eq can be estimated as

$$t_\mathrm{eq} = \sqrt{\frac{2\pi T_\mathrm{max}^2}{T_\mathrm{a}|T''_{tt}(t_0)|}}. \quad (3)$$

Here, $T''_{tt} = \partial^2 T/\partial t^2$. Thus, having found the dependence of the film temperature on time at each film point, one can determine the structure of the oxide formed.

Subsequent etching of the film forms its topology as a result of removal of the film portions that were not protected by a sufficiently thick oxide layer. The exact value of this critical thickness is unknown. According to different sources, it ranges from 4 to 8 nm. To determine the upper limit for the minimum width of elements formed in the laser-produced oxide film, we assumed the critical thickness to be 6 nm in our calculations.

In this study the emphasis was on the increase in the resolution of the microstructure formation by scanning a cw laser beam. In this case, the irradiation time is several orders of magnitude longer than in the case of conventional nanosecond irradiation.

3. Analysis of the limiting resolution of the thermochemical image recording

Let us consider the possibility of obtaining a thermochemical image of minimum sizes on a film for the laser radiation intensity in the focal spot described by a Gaussian distribution. The thickness of the oxide layer that is formed on a metal surface as a result of exposure to a rectangular laser pulse of width τ and in accordance with the Wagner oxidation law, as follows from expressions (2) and (3), can be written in the form [13]

$$H = 2\left[\frac{BT_\mathrm{max}^2\tau}{T_\mathrm{a}(T_\mathrm{max} - T_\mathrm{in})}\right]^{1/2}\exp\left(-\frac{T_\mathrm{a}}{2T_\mathrm{max}}\right), \quad (4)$$

where T_in is the initial temperature. Hence, the ratio of the oxide layer thicknesses at a distance r from the centre of the irradiated region (H_r) and in its centre (H_0) is determined by the formula

$$\frac{H_\mathrm{r}}{H_0} = \frac{T(r)}{T(r=0)}\left[\frac{T(r=0) - T_\mathrm{in}}{T(r) - T_\mathrm{in}}\right]^{1/2} \times \exp\left[-\frac{T_\mathrm{a}}{2T(r)} + \frac{T_\mathrm{a}}{2T(r=0)}\right]. \quad (5)$$

On the assumption that $T(r)/T(r=0) \approx \exp[-(r/r_0)^2]$ and $T - T_\mathrm{in} \approx T$, we find the ratio of the characteristic size r of the image element formed on the film to the radius of the irradiated area for the case $r < r_0$:

$$\frac{r}{r_0} \approx \sqrt{2\frac{T_0}{T_\mathrm{a}}\ln\frac{H_0}{H_\mathrm{r}}}, \quad (6)$$

where $T_0 \approx 1220$ K is the temperature that is sufficient (according to the experimental data) to form a protective oxide layer on a chromium film.

Thus, the minimum size of the image element on a film, which can be formed by laser oxidation with subsequent etching, depends on the size of the irradiated area and is determined by the oxide properties and etching conditions. In particular, at $H_\mathrm{r}/H_0 = 0.8$, the minimum element size r_min is $\sim 0.1r_0$. This means that the element size can be in principle much smaller than the focal spot radius and, correspondingly, much smaller than the radiation wavelength.

4. Oxidation of chromium film under a scanning cw laser beam

To find the oxide layer thickness according to expressions (2) and (3), it is necessary to determine the temperature field in the metal film during its exposure to a scanning laser beam. Let us consider the heating of a metal film of thickness h, located on a dielectric substrate, by a scanning cw laser beam with a Gaussian intensity distribution. Note that during scanning the temporal shape of the pulse, which affects each surface point, depends on the spatial intensity distribution in the beam. We will consider the case of quasi-stationary heating. Previously we estimated the ratio of the thermal flux from the irradiated region in the film, P_1, to the thermal flux into the substrate, P_2:

$$\frac{P_1}{P_2} = \frac{2h}{r_0}\sqrt{\frac{a}{a_\mathrm{s}}}, \quad (7)$$

where r_0 is the radius of the irradiated area on the film surface, a is the film thermal diffusivity, and a_s is the substrate thermal diffusivity. For most cases of practical importance, $P_1/P_2 > 1$. In particular, for a 100-nm-thick chromium film on a glass K-8 substrate, at an irradiated-

area radius of 0.25 μm, $P_1/P_2 \approx 4$. Thus, the laser-heated film can be considered as adiabatically isolated, with disregarded heat removal into the substrate.

The heat conduction equation for a film heated uniformly over its thickness has the form

$$\frac{\partial T}{\partial t} - a\left(\frac{\partial^2 T}{\partial x^2} + \frac{\partial^2 T}{\partial y^2}\right) = \frac{P(1-R)}{\pi r_0^2 \rho c h} \exp\left[-\frac{(x-Vt)^2 + y^2}{r_0^2}\right], \quad (8)$$

where P is the laser power; V is the scanning velocity; and ρ, c, and R are, respectively, the density, specific heat, and reflectance of the film. The x and y axes lie in the film plane, and the x axis coincides with the scanning direction and passes through the centre of the irradiated region.

The solution to Eqn (8), which was obtained by us as a result of passing to a moving coordinate system, linked to the irradiated region, and applying the zero-order Hankel transform to this equation, was reported in [11]. The numerical calculations showed that the relative decrease in the oxide layer thickness to the periphery of the intensity distribution in the focal spot is much smaller than the relative decrease in the maximum attainable temperature (it is shown in Fig. 1 for a particular case where the temperature in the spot centre reaches 1600 °C). As a result, one can obtain a resolution of thermochemical recording better than the spatial resolution of focusing optics.

A characteristic feature of the curve in Fig. 1, which describes the distribution of the oxide layer thickness in the direction perpendicular to the scanning direction, is its significant deviation from Gaussian: the plateau at 0 – 0.05 μm from the spot centre is followed by a portion with a sharp decrease in the oxide layer thickness at large distances from the centre. Mathematically, the boundary between these portions is determined by the position of the point y^*, where the second derivative of the function $H(y)$ [or $I(y)$] is zero. For the function $H(y)/H(0)$ in Fig. 1, $y^* \approx 0.05$ μm, whereas for the Gaussian intensity distribution $I(y)$ in the focal spot $y^* = r_0/\sqrt{2} \approx 0.36$ μm and for the temperature distribution $y^* \approx r_0/\sqrt{2} + \sqrt{a r_0/V} \approx 0.4$ μm.

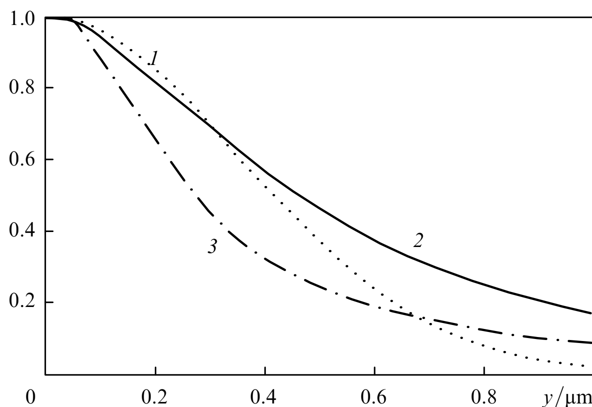

Figure 1. Dependences of the relative changes in the (1) intensity [$I(y)/I(0)$], (2) temperature [$T_{max}(y)/T_{max}(0)$], and (3) oxide film thickness [$H(y)/H(0)$] on the distance from the laser beam centre; $h = 100$ nm, $r_0 = 0.5$ μm, $T_{max}(0) = 1600$ °C, $H(0) = 8$ nm.

The calculated width of the image obtained (on the assumption that the critical oxide layer thickness, corresponding to the image edge, is 6 nm) for an irradiated area 0.5 μm in diameter ranges from 0.4 μm at the minimum radiation powers and maximum scanning velocities (Fig. 2, bottom curve) to 2.5 μm at the melting threshold (Fig. 2, top curve). With adequately chosen radiation power (in correspondence with the scanning velocity), the minimum width of the image obtained barely depends on the scanning velocity, and the resolution is in the range from 2500 to 400 mm^{-1}.

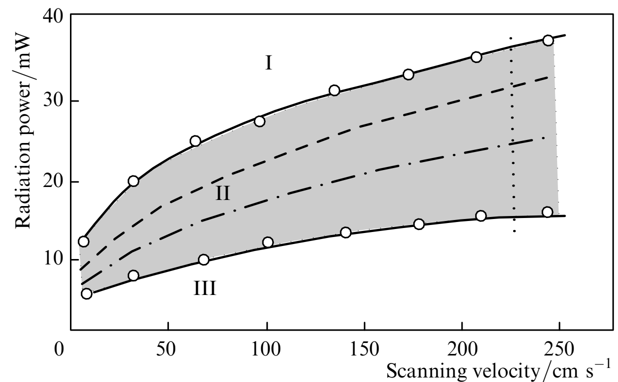

Figure 2. Dependence of the thermochemical recording range on the irradiation conditions: (I) melting range, (II) thermochemical range, and (III) the range of insufficient oxide layer thickness. The dashed and dot-dashed lines are the calculated boundaries between ranges I and II and between ranges II and III, respectively ($h = 100$ nm).

The calculations performed showed that the radiation power that is necessary to oxidise a 100-nm chromium film is in the range of 10 – 20 mW at a scanning velocity ranging from 0.1 to 1 m s^{-1} and the focal spot radius $r_0 \sim 0.4$ μm, which is in good agreement with the experimental values: 10 – 30 mW. Depending on the scanning velocity, the radiation power should be changed so as to provide an oxide film thickness exceeding the required critical value and, at the same time, to exclude melting. The calculated and experimentally found ranges of allowable values of recording beam power, depending on the scanning velocity, are presented in Fig. 2.

5. Experimental study

The spatial resolution during thermochemical recording was experimentally studied on a precise laser system developed at the Institute of Automation and Electrometry, Siberian Branch, Russian Academy of Sciences (Novosibirsk) [8, 14]. A substrate with a thin chromium film was installed on the top part of a precise aerostatic spindle (rotation speed up to 15 rps). The power of a cw argon laser ($P \sim 0.5$ W, $\lambda = 488$ nm) was controlled by a computer with a 10-bit resolution. The laser beam was focused into a spot 0.6 μm in diameter (at the half-intensity level). The optical head was moved in the radial direction over aerostatic guides using a linear motor and an interferometric coordinate feedback. The displacement range was 250 mm, the error in positioning was about 20 nm, and the positioning resolution was better than 1 nm^{-1}.

The experiments were performed with chromium films 80 – 100 nm thick, deposited on fused quartz and optical

glass substrates. The films obtained by both thermal deposition and magnetron sputtering were analysed. During exposure the scanning velocity with respect to the substrate was varied from 4 to 180 cm s^{-1}. This range corresponds to the range of the radii of circular beam trajectories from 0.5 to 30 mm at a rotation speed of about 10 rps. After the exposure the film was processed in a selective etchant (etching time of about 3 min) [14], composed of six parts of 25 % $K_3Fe(CN)_6$ solution and one part of 25 % NaOH solution.

An important question is the thickness of the oxide film formed during exposure. We performed direct thickness measurement using a Talystep profilograph. Figure 3a shows a micrograph (recorded in the reflection geometry) of the chromium film surface before etching, with a series of recorded test lines. The recording beam power was successively reduced from line to line. Figure 3c shows a micrograph of the same surface portion after etching. Figures 3b and 3d present the profilograms of this portion

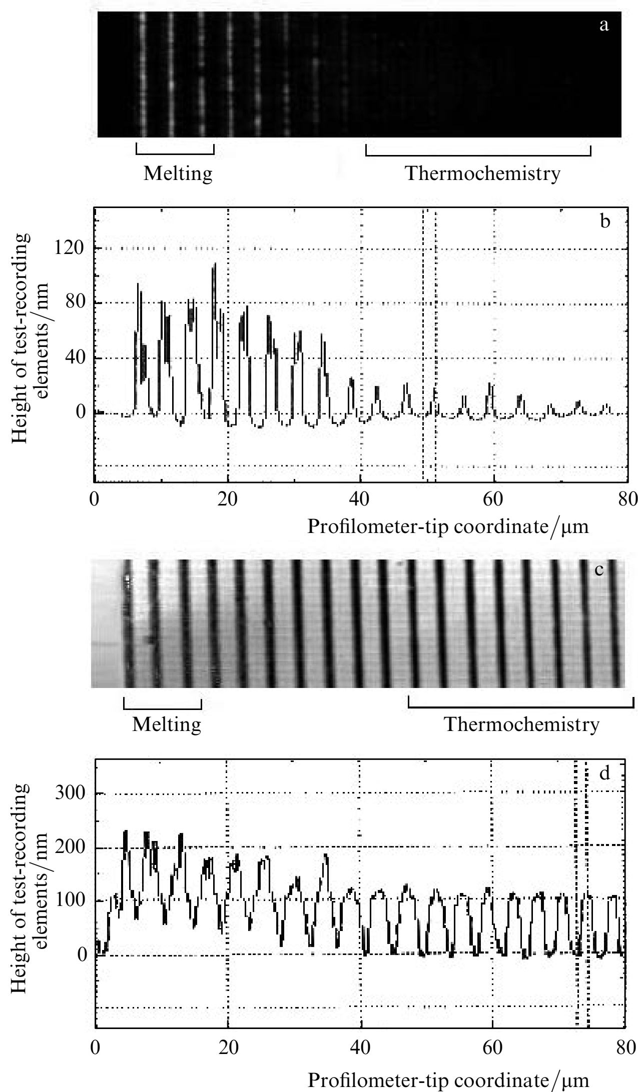

Figure 3. Microphotographs and the corresponding profilograms for a fragment of test recording on a chromium film (a, b) before and (c, d) after etching. The 100-nm-thick chromium film was obtained by thermal deposition. The track repetition period is 4 μm. The film velocity during recording is 80 cm s^{-1}.

of the chromium film before and after etching. It can be seen that, before etching, the change in the relief height reaches 100 nm in the range of film melting and decreases from 50 to 10 nm in the range of hidden-image formation (thermochemistry range). The data in Fig. 3b suggest that the maximum oxide film thickness does not exceed the initial thickness of the chromium film. This result is in agreement with the classical theory, because the volume of the oxide formed (Cr_2O_3) exceeds that of the initial material (Cr) by a factor of about 2. In the range of thermochemical recording the oxide film thickness amounts to 10 – 20 nm and then gradually decreases, in correspondence with the accepted model.

The dependence of the line width on the exposing radiation power was investigated using an optical microscope and a Solver Pro atomic-force microscope (AFM). Figure 4 shows a micrograph of the test sample, recorded on a chromium film (recording area radius 20 mm, velocity 150 cm s^{-1}). The distance between the lines (tracks) is 1.5 μm. The gap between groups of lines is 1 μm in the radial direction. The beam power increased from bottom to top. The width of the recorded tracks depends linearly on the laser power (Fig. 5); the maximum resolution is 650 lines mm^{-1}.

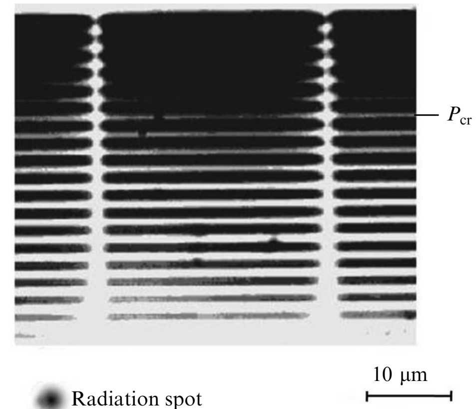

Figure 4. Microphotograph of a test sample (40 × 40 μm), recorded on a chromium film; P_{cr} is the critical power (at which the film starts melting).

The track profiles at different radiation powers are shown in Fig. 6. It can be seen that at a sufficiently low power the track has a shape of a narrow peak (width 0.4 μm at a level of 0.5), whereas the radiation spot (Fig. 4, left bottom corner) has a much larger diameter (0.6 μm at a level of 0.5) and a Gaussian-like intensity distribution. These experimental data confirm the theoretical results presented in Fig. 1.

Figure 7 shows the experimental dependences of the spatial resolution on the recording spot velocity with respect to the film and, for comparison, the characteristic exposure time. The curves are given for the films of two types, obtained by thermal deposition and magnetron sputtering. The microstructure of the thermally deposited films are characterised by a lower resolution because of the formation of microcrystallites (recrystallisation) at the line edges. This factor is especially important for low exposure times.

For the films deposited by magnetron sputtering, the spatial resolution in the case of high scanning velocities

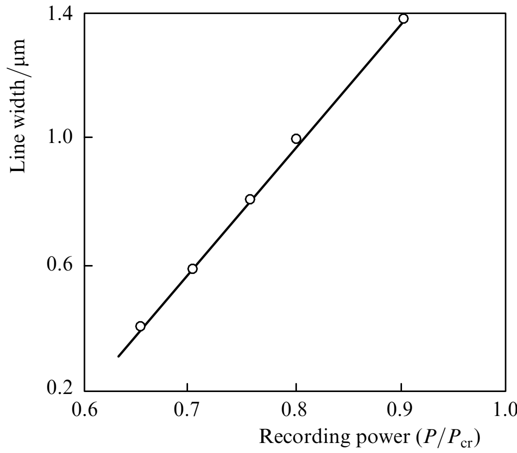

Figure 5. Dependence of the width of recorded tracks on the recording beam power.

exceeds 1600 mm^{-1}, a value close to the limiting resolution of an optical recording system. At velocities below 30 cm s^{-1} the resolution deteriorates: the temperature distribution in the film expands due to the thermal conduction.

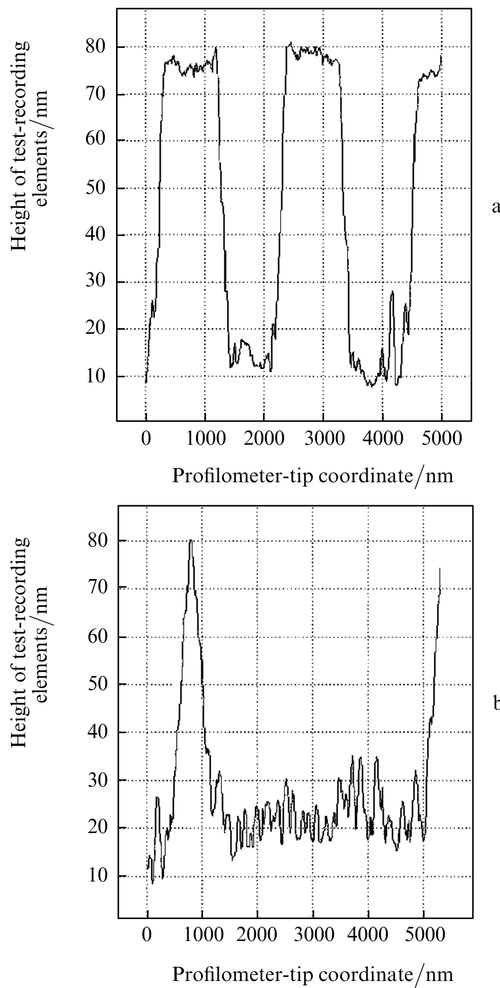

Figure 6. AFM profiles of tracks with widths of (a) 0.9 and (b) 0.2 μm on a chromium film.

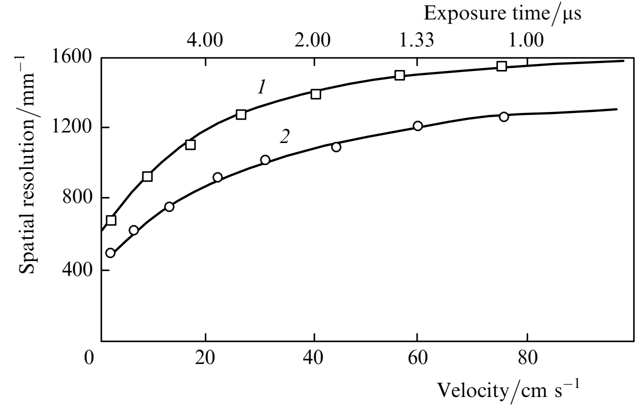

Figure 7. Dependences of the spatial resolution $\delta = 1/2d$ (d is the minimum width of a recorded line) during image recording on the scanning velocity and the corresponding exposure time: (*1*) magnetron sputtering, chromium film thickness 50 nm, and (*2*) thermal deposition, film thickness 80 nm.

6. Results and discussion

Our theoretical and experimental studies showed that the surface oxidation makes a significant contribution to the formation of a structure in a chromium film by LTT. Along with the surface oxidation of the chromium film, some other effects occur in the film bulk.

The changes occurring in the film bulk are evidenced by the results of studying the etching kinetics in the irradiated and unirradiated chromium films (Fig. 8) by the photometric method [15]. It can be seen in Fig. 8 that the beginning of etching of both irradiated and unirradiated films is characterised by a time delay (t_1 and t_3, respectively), which is due to the presence of chromium oxides. The thickness of the native oxide layer on the surface of the unirradiated film is 1 – 2 nm; during irradiation this value increases to 10 – 20 nm, as a result of which the etching time of this layer increases from 20 to 100 s. However, this process barely affects the film transmission. The structural changes that occur in thin films during laser irradiation change their physical properties (in particular, the growth of microcrystallites, the change in the number of lattice defects [14], and bulk oxidation) and, finally, reduce the etching

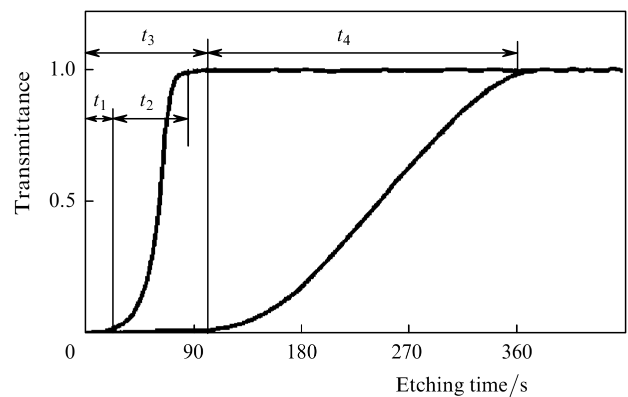

Figure 8. Typical dependences of the transmittances of (*1*) unexposed 100-nm-thick chromium film and (*2*) the same film exposed at a wavelength of 633 nm on the etching time [$K_3Fe(CN)_6$ and NaOH solutions].

rate. Note that the etching time t_4 of the irradiated film exceeds the etching time t_2 of a pure chromium film of the same thickness by a factor of 2.5.

Along with the difference in the etching rates, we should indicate the significant tilt of the boundary between the exposed and etched regions (Fig. 6b). One can see that the width of the peak base is about 500 nm for a film 80 nm thick; i.e., the tilt angle is $\sim 15^{\circ}$, whereas it would be much larger if only oxidation occurred [5].

The detailed study of this process is especially important for preparing DOEs using LTT, because specifically the surface of the chromium film (and, correspondingly, element) interacts with light. For example, when fabricating a reflective DOE, the etching time should be in the range from t_2 to t_3 (Fig. 8), because in the opposite case both the thickness and reflectance of the chromium film will decrease.

7. Conclusions

(i) It was shown theoretically that the resolution $\delta = 1/2d$ of a thermochemical image exceeds that of a temperature image due to the inverse exponential dependence of the oxide growth rate on temperature. The gain in the resolution, which is determined by the ratio of the first derivatives with respect to the coordinate $(1/H)|\partial H/\partial x|$ and $(1/T)|\partial T/\partial x|$ reaches 20 in our case. The true (experimental) resolution of the thermochemical image formation can be even higher due to the photothermochemical feedback between the absorbed power density, oxide thickness, and temperature.

(ii) The possibility of thermochemical formation of film structures with a high spatial resolution upon local heating by a scanning focused cw laser beam was studied both theoretically and experimentally. It was shown that this mode can be used to form high-quality diffraction structures with a spatial frequency up to 650 mm^{-1} and higher, at the focusing objective numerical aperture $\text{NA} = 0.65$, laser radiation wavelength 488 nm, and beam scanning velocity more than 100 cm s^{-1}.

(iii) Both the theoretical (model) and experimental limiting resolutions depend on the minimum thickness of oxide film that is stable to etching.

Acknowledgements. This study was supported by the Russian Foundation for Basic Research (Grant Nos 09-02-01065 and 10-02-00208) and by State Contract No. P1134.

References

1. Veiko V.P., Kotov G.A., Libenson M.N., Nikitin M.N. *Dokl. Akad. Nauk SSSR*, **208**, 587 (1973).
2. Koronkevich V.P., Poleshchuk A.G., Churin E.G., Yurlov Yu.I. *Kvantovaya Elektron.*, **12** (4), 755 (1985) [*Sov. J. Quantum Electron.*, **15** (4), 494 (1985)].
3. Soifer V.A. (Ed.) *Metody komp'yuternoi optiki* (Methods of Computer Optics) (Moscow: Fizmatlit, 2003).
4. Burge J.H. *Proc. SPIE Int. Soc. Opt. Eng.*, **2576**, 258 (1995).
5. Moro W. *Mikrolitografiya: printsipy, metody, and materialy* (Microlithography: Principles, Methods, Materials) (Moscow: Mir, 1990).
6. Poleshchuk A.G., Churin E.G., Koronkevich V.P., Korolkov V.P. *Appl. Opt.*, **38**, 1295 (1999).
7. Bunkin F.V., Kirichenko N.A., Luk'yanchuk B.S. *Izv. Akad. Nauk SSSR, Ser. Fiz.*, **45** (6), 1018 (1981).
8. Poleshchuk A.G., Korol'kov V.P., Cherkashin V.V., Reichelt S., Burge J. *Avtometriya*, 3, 3 (2002).
9. Chen C.G., Konkola P.T., Heilmann R.K. et al. *Proc. SPIE Int. Soc. Opt. Eng.*, **4936**, 126 (2002).
10. Mallik P.C.V., Zehnder R., Burge J.H., Poleshchuk A. *Proc. SPIE Int. Soc. Opt. Eng.*, **6721**, 672104 (2007)
11. Veyko V.P., Shakhno E.A., Poleshchuk A.G., Korolkov V.P., Matyzhonok V. *J. Laser Micro/Nanoengineering*, **3** (3), 201 (2008).
12. Kotov G.A., Libenson M.N. *Electron. Tekh. Ser.*, **6**, 4 (44), 56 (1973).
13. Libenson M.N. *Lazernooindutsirovannye opticheskie i termicheskie protsessy v kondensirovannykh sredakh i ikh vzaimnoe vliyanie* (Laser-Induced Optical and Thermal Processes in Condensed Media and Their Mutual Effect) (St. Petersburg: Nauka, 2007) p. 423.
14. Tochitskii E.I. *Kristallizatsiya i termoobrabotka tonkikh plenok* (Crystallisation and Heat Treatment of Thin Films) (Minsk: Nauka i tekhnika, 1976).
15. Cherkashin V.A., Churin E.G., Burge J.H., Korolkov V.P., Poleshchuk A.G., Kharisov A.A., Koronkevich V.P. *Proc. SPIE Int. Soc. Opt. Eng.*, **3010**, 168 (1997).